



Original Research

Three-Dimensional Rotational Angiography to Guide Cardiac Catheterization in Critical Infants Below 5kg of Body Weight

Chenise N. Lucas, MSc^{*}, Martijn G. Sliker, PhD, Mirella M.C. Molenschot, MD, Hans M.P.J. Breur, PhD, Gregor J. Krings, PhD

Department of Pediatric Cardiology, Wilhelmina Children's Hospital, University Medical Center of Utrecht, Utrecht, the Netherlands

ABSTRACT

Background: Three-dimensional rotational angiography (3DRA) is a promising advancement to guide cardiac catheterizations. It is used with restraint in critically ill infants with congenital heart disease (CHD) due to the lack of research conducted within this patient group.

Methods: Data of all infants with CHD and a body weight <5 kg who underwent cardiac catheterization with the use of 3DRA between November 2011 and April 2021 were retrospectively analyzed. Primary outcome measures were 3DRA-related periprocedural deaths or major adverse events (MAEs). Secondary outcome measures were 3DRA-related minor adverse events (MiAEs), the amount of radiation exposure and contrast agent, and whether 3DRA led to important new findings. The case-based workflow of 3DRA in vulnerable infants is explained.

Results: Eighty-six patients underwent 109 cardiac catheterizations in which 132 3DRA scans were performed. Median age and weight were 50.0 days (IQR, 20.0-98.5) and 3.8 kg (IQR, 3.2-4.5). There were no periprocedural deaths or MiAEs, and only 2 MAEs occurred, both concerning ventricular fibrillation. The median radiation exposure was 160.0 cGy·cm² (IQR, 81.3-257.5), of which 28.0 cGy·cm² (IQR, 19.4-43.0) was derived from 3DRA. The mean amount of contrast agent used was 4.8 ± 1.6 mL/kg. In 70.6%, 3DRA imaging led to important new findings. Multivariate binary logistic regression analysis showed the presence of comorbidity to be associated with a lower odds of receiving a 3DRA-derived radiation dose ≥15 cGy·cm² (*P* = .01). Additionally, the interval between surgery and cardiac catheterization was significantly associated with higher odds of a contrast dye consumption ≥6 mL/kg (*P* = .046).

Conclusions: 3DRA proved to be safe in vulnerable infants with CHD weighing <5 kg, enabling visualization of anatomical substrates often invisible in conventional angiography. However, when an advanced computed tomography scanner is available, the diagnostic purposes for 3DRA are few. The greatest benefit of 3DRA usage is interventional guidance (3D roadmap).

Introduction

Congenital heart disease (CHD) is the most frequent birth defect, and the reported prevalence at birth has rapidly increased over the past decade.¹ Approximately 6 to 8 newborns of every 1000 live births have CHD.² Over the past years, both diagnostic and therapeutic possibilities have improved tremendously, among them cardiac catheterization, leading to a significant decrease in mortality.³

Three-dimensional rotational angiography (3DRA) is an advanced imaging technology applied during cardiac catheterization. This technique provides imaging of complex anatomy with high spatial resolution and enables 3D procedural guidance.^{4,5} Additionally, the 3DRA images can be fused with computed tomography angiography (CTA) images.⁶

Although there is no literature available on the usage of 3DRA in infants with CHD with <5 kg of body weight, this group of small infants with complex lesions may benefit significantly from 3DRA while undergoing cardiac catheterization. Despite evidence of the superior imaging quality of 3DRA,^{6,7} the technique is used with restraint in neonates and small infants considering their often critical condition. There are also concerns about the potentially deleterious effects of inadequate radiation exposure and the larger amount of contrast agent applied compared with conventional angiography.⁷

A large number of newborns with CHD have to undergo cardiac catheterization within the first weeks after birth, often related to residual lesions following previous cardiac surgery. Due to exceedingly complex anatomy in most of these infants, cardiac catheterization using conventional biplane cine-angiography can be challenging or even

Abbreviations: 3DRA, 3-dimensional rotational angiography; CHD, congenital heart disease; HLHS, hypoplastic left heart syndrome; MAE, major adverse event; MiAE, minor adverse events; PA VSD, pulmonary atresia with ventricular septal defect; RVP, rapid ventricular pacing; TOF, tetralogy of Fallot.

Keywords: 3-dimensional rotational angiography; cardiac catheterization; congenital heart disease; infant; pediatric cardiology.

^{*} Corresponding author: cheniselucas@gmail.com (C. Lucas).

<https://doi.org/10.1016/j.jscai.2024.102391>

Received 8 June 2024; Received in revised form 9 September 2024; Accepted 11 September 2024

2772-9303/© 2024 The Author(s). Published by Elsevier Inc. on behalf of the Society for Cardiovascular Angiography & Interventions Foundation. This is an open access article under the CC BY-NC-ND license (<http://creativecommons.org/licenses/by-nc-nd/4.0/>).

insufficient in depicting the ideal angulation and anatomical interaction. In these complex cases, 3DRA could be beneficial.

The purpose of this study is to analyze the utility, safety, and value of 3DRA in cardiac catheterizations in children with CHD and a body weight of ≤ 5 kg. This paper represents the 10-year experience with 3DRA in a single center.

Methods

Study design and population

This single-center, descriptive cohort study retrospectively enrolled all patients who underwent cardiac catheterization with 3DRA at the children's heart center of University Medical Center in Utrecht between November 2011 and April 2021. Inclusion criteria were CHD and a body weight ≤ 5 kg.

Collected demographic data included age (days), weight (kilograms), sex, comorbidities, and cardiac diagnosis (type of CHD), as well as survival at follow-up. Catheterization data included procedure duration, fluoroscopy time, type of intervention, state of the procedure (emergency or elective), the interval between previous surgery and catheterization, and the indication for cardiac catheterization (diagnostic or interventional). In addition, the amount of contrast dye consumption, radiation exposure, application of rapid ventricular pacing (RVP), and occurrence of complications were analyzed.

Patients were divided into 4 diagnostic categories: hypoplastic left heart syndrome (HLHS), aortic lesions, tetralogy of Fallot (TOF), and others. Hypoplastic left heart complex, coarctation of the aorta, and hypoplasia of the aortic arch were combined in the category "aortic lesions." TOF, double outlet right ventricle (right ventricle), Taussig-Bing anomaly, and pulmonary atresia with ventricular septal defect (PA VSD) were combined in the category "TOF." All other diagnoses were combined under the name "diverse."

Primary outcomes were any 3DRA-related major adverse events (MAEs), defined as death or life-threatening complications that required immediate intervention, such as surgery or cardiopulmonary resuscitation. Secondary outcomes were 3DRA-related minor adverse events (MiAEs), the amount of contrast dye used, radiation exposure, and additional anatomical information provided by 3DRA. MiAEs were defined as any non-life-threatening complications related to 3DRA. Radiation exposure was measured and reported as dose area product (DAP).⁸

3DRA

All patients underwent initial 3DRA on a biplane angiographic system (Artis Zee with Syngo DynaCT, Siemens Healthineers), with 200° rotation of the frontal C-arm around the patient.⁹ A 5-second rotational angiography was performed under RVP, respiratory arrest, and contrast (Omnipaque 300, GE Healthcare) injection in 1 or multiple locations. The region of interest in the computed tomography (CT) was postprocessed by adapting for the Hounsfield unit ranges and removing redundant tissue to optimize visualization of the anatomical region of interest.⁹ In interventional procedures, the adapted images were subsequently projected onto the real-time frontal 2D angiographic system to function as 3D guidance. If necessary, noncontrast 3DRA was performed to investigate airway to stent interactions.

Setup and timing of contrast injection during rotational angiography

Contrast injection parameters (amount and flow, timing, concentration, and location) in rotational angiography differ substantially from regular biplane angiography. During the C-arm rotation

(depending on the vendor, from 4-5 seconds), contrast distribution and density should be constant. In our 3DRA workflow, the amount of contrast used is calculated based on flow in mL/s. In infants weighing 3 kg, each circuit receives a flow of 2 mL/s, which can be increased to 4 mL/s in infants weighing 5 kg. The timing of contrast injection and rotational angiography is crucial to account for differences in contrast distribution and blood flow. Contrast is injected in the cavity proximal to the region of interest 1 second (systemic circulation) or 2 seconds (pulmonary circulation) before the rotational angiography is initiated. This guarantees equal contrast distribution in the high-flow systemic and low-flow pulmonary circuit. Through dilution of contrast with 60% NaCl 0.9%, the absolute amount of contrast applied in critically ill infants weighing <5 kg is reduced to the approximate amount of contrast used in 2 conventional angiographies. The possible contrast injection locations, amount, flow, and timing of the injection are shown in Figure 1 with the corresponding cases of 3D guided interventions shown in Figure 2. RVP is applied to decrease blood pressure and retard contrast circulation. Ventilation should be paused to reduce movement artifacts.

In cases of HLHS with Sano shunt stenosis (Figures 1 and 2A), single location contrast injection using an injector is sufficient because the cavity (RV) proximal to the region of interest (Sano shunt) serves as a contrast depot without the risk of contrast washout to other regions. Double contrast volume and flow (Figure 1A, 12 mL at 4 mL/s) is necessary considering the doubled cardiac output of the single RV in stage I hemodynamics. Contrast is injected 1 second before rotational angiography is initiated (1-second X-ray delay). In a biventricular situation (Figures 1 and 2B), 12 mL of contrast with a flow rate of 2 mL/s is manually injected into the RV followed by contrast injection in the left ventricle (LV) 1 second later (12 mL at 2 mL/s). The rotational angiography is initiated 2 seconds after contrast injection in the RV and 1 second after the LV. In single ventricle situations (Figures 1 and 2C) with pulmonary circulation depending on a duct, aortopulmonary shunt, or major aortopulmonary collateral arteries, dual contrast injection is performed. The dominant (single) ventricle is filled manually with contrast (12 mL at 2 mL/s) while simultaneously injecting additional contrast into the ascending aorta (12 mL, 2 mL/s) to enable visualization of the high-flow duct, shunt, or major aortopulmonary collateral artery perfusion. The rotational angiography is initiated with a 1-second x-ray delay. Postprocessing of a 3D volume data set depends on individual expertise, procedural workflow, and quality of the rotational angiography.

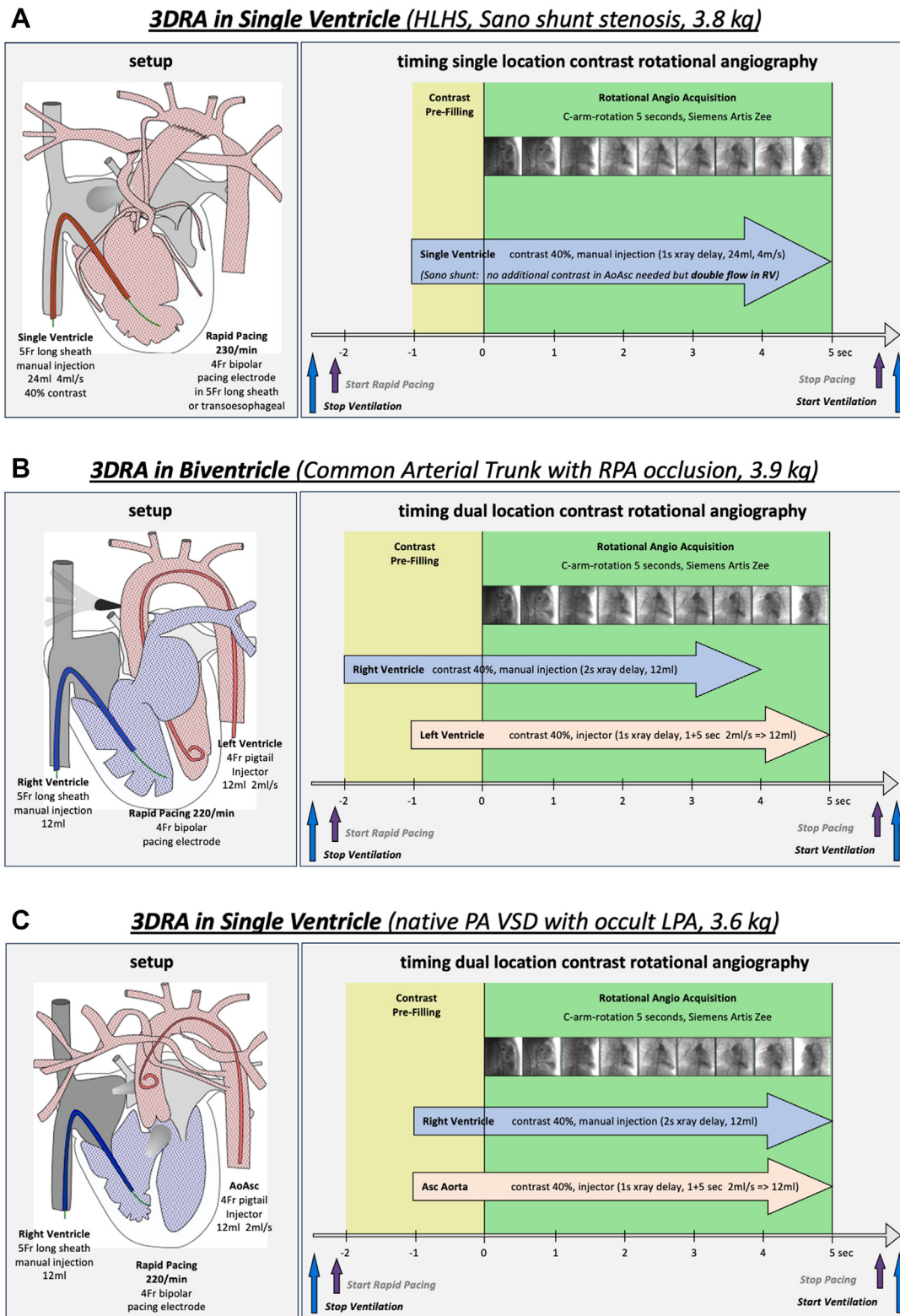
Statistical analysis

All statistical analyses were performed using IBM SPSS Statistics version 26.0 (IBM Corp). Continuous variables are presented as median and IQR or as mean and SD, as appropriate based on the Kolmogorov-Smirnov test. Categorical variables are presented as percentages and/or count. Procedural changes over time were analyzed using descriptive frequency statistics.

Multivariate binary logistic regression analysis was used to test for predisposing factors affecting outcomes. Continuous variables were dichotomized into appropriate variables. Analyses with a *P* value $< .05$ were considered statistically significant.

Ethical statement and informed consent

This research was conducted in accordance with the ethical standards of our organization. Written parental informed consent was obtained for all patients.

**Figure 1.**

Setup and timing of contrast injection, rapid pacing, and ventilation stop in 3 cases with complex substrates in infants weighing <5 kg. (A) Single location contrast injection in HLHS to visualize the Sano shunt and RPA/LPA stenosis; double contrast flow (4 mL/s) considering the doubled cardiac output of the single ventricle in stage I; 1 s contrast prefilling before start of the rotational angiography. (B) Dual location contrast injection in biventricular hemodynamics: manual injection of contrast in the RV 2 s before rotational angiography to optimize contrast distribution (12 mL) through 5F long sheath; LV injection by injector with 12 mL of contrast and a flow of 2 mL/s 1 s before rotational angiography; rapid pacing via long sheath or transesophageal. (C) Dual location contrast injection in single ventricle with duct, shunt, or major aortopulmonary collateral artery-dependent pulmonary artery flow: manual injection of 12 mL of contrast in the RV 1 s before rotational angiography; additional aortic contrast injection by injector with 12 mL of contrast and a flow of 2 mL/s 1 s before rotational angiography to support aorto-to-pulmonary contrast distribution. 3DRA, 3D rotational angiography; AoAsc, ascending aorta; HLHS, hypoplastic left heart syndrome; LPA, left pulmonary artery; LV, left ventricle; PA VSD pulmonary atresia with ventricular septal defect; RPA, right pulmonary artery; RV, right ventricle.

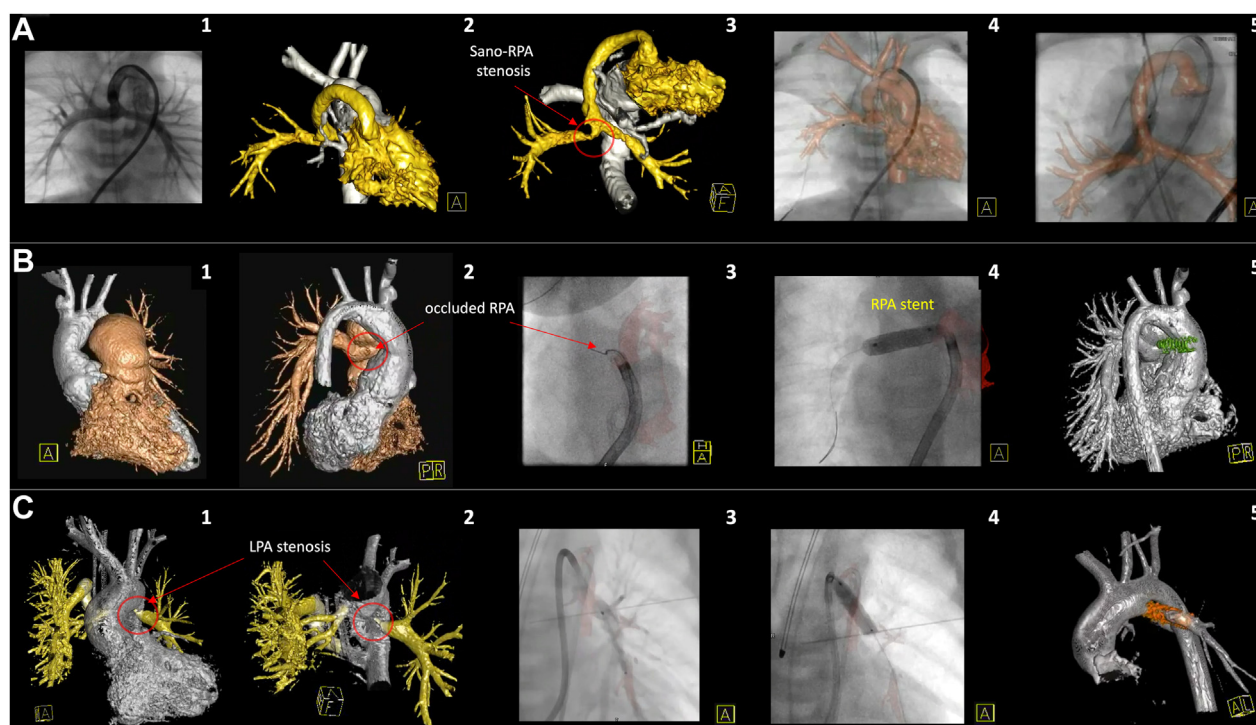


Figure 2.

Use of 3DRA in 3 critical infants weighing <5 kg. (A) Infant with hypoplastic left heart syndrome, 3.8 kg, SaO₂ 50%, 10 days after Norwood procedure with Sano shunt. Sano-RPA stenosis not visible in biplane angiography (A1) but clearly identified through 3DRA in caudal view (A3). Coronary stent implantation (4.5 × 14 mm) using 3DRA guidance (A4, A5). (B) Infant with common arterial trunk, 3.9 kg, 6 weeks after correction (RPA arising from brachiocephalic trunk, LPA from common trunk) by direct LPA-to-RV anastomosis and RPA side-to-LPA anastomosis, supra systemic RV pressure, occult RPA (B1). 3DRA demonstrates the RPA occlusion at ostium level (B2). Recanalization using 3DRA guidance with an Oscor steerable 7F sheath and 5F telescope (5F JR coronary guide catheter, 4F MP 120 cm, 2.6F microcatheter, and Teflon-tipped coronary guide wire) (B3). Implantation of a Cook Formula 418 stent 8 × 20 mm using an Advance balloon 5 × 20 mm (B4). Result with projection of the implanted stent on the initial 3DRA image (B5). (C) Infant with pulmonary atresia with ventricular septal defect, 3.6 kg. Absence of native PA system (C1/2). RPA perfusion through large collateral artery. LPA connected to severely stenotic patent ductus arteriosus under high dose prostaglandins. Sheathless telescopic transductal approach (5F coronary guide catheter, 4F MP 120 cm, Teflon-tipped coronary guide wire [C3]) and implantation of a 4 × 14 mm coronary stent. Projection of the implanted stent on the initial 3DRA image (C5). 3DRA, 3-dimensional rotational angiography; LPA, left pulmonary artery; PA, pulmonary artery; RPA, right pulmonary artery; RV, right ventricle; SaO₂, oxygen saturation of arterial blood.

Results

Demographic data

Between November 2011 and April 2021, 86 patients with weighing ≤5 kg underwent 109 cardiac catheterization procedures in which 132 3DRA scans were performed. Of these patients, 65.1% were male. Median age and weight at the time of the procedure were 50.0 days (IQR, 20.0-98.5) and 3.8 kg (IQR, 3.2-4.5), respectively. In 20 patients, 2 3DRA scans were performed during 1 procedure, mostly to evaluate the intervention. One patient underwent 4 3DRA scans after a Norwood procedure. The initial 3DRA image showed severe aortopulmonary shunt stenosis after which balloon dilation was performed, which resulted in severe aneurysm formation. During bail-out treatment, 3 subsequent 3DRA scans were performed to monitor the results of the stepwise approach.

HLHS was the most frequent cardiac diagnosis, with a prevalence of 19 (22.1%). PA VSD was the second most frequent diagnosis, followed by hypoplastic left heart complex and TOF. The most common comorbidities were genetic syndromes, with a prevalence of 21 (24.4%). The overall demographic data are summarized in Tables 1 and 2.

Of the procedures, 47 (43.1%) were diagnostic and 62 (56.9%) were interventional. Fifty-four (49.5%) emergency cardiac catheterizations were performed, of which 16 were diagnostic and 36 interventional. The other 55 (50.5%) cardiac catheterizations were performed electively, of which 31 were diagnostic and 24 interventional. The most frequent procedures were stent implantation (36 cases, 58.1%), followed by balloon dilation (11 cases, 17.7%).

Fifty-nine (54.1%) procedures were preceded by surgery with a mean interval of 47.6 ± 36.5 days. Femoral vascular access was chosen in 93.3%, with use of 4F and 5F sheaths. In the cross-sectional follow-up point in May 2021, 21 (24.4%) patients had died. The procedural data are summarized in Table 3.

Complications

Two 3DRA-related complications (MAEs) occurred during the 109 procedures (1.8%). In both cases, ventricular fibrillation (VF) was triggered by RVP and associated with severely reduced RV function and high pressure load. Cardiopulmonary resuscitation was successful.

Radiation, contrast, and rapid ventricular pacing

The median amount of total radiation exposure during the procedures was 160.0 cGy·cm² (IQR, 81.3-257.5), of which a median amount of 28.0 cGy·cm² (IQR, 19.4-43.0) was derived from 3DRA. Expressed as percentages, 21.1% of radiation exposure during the cardiac catheterizations was derived from 3DRA. When examined as DAP per kilogram body weight, there was a median DAP of 43.1 cGy·cm²/kg (IQR, 19.6-70.6) in the complete procedure and 7.1 cGy·cm²/kg (IQR, 5.0-11.5) derived from 3DRA. The mean percentage of radiation exposure derived from 3DRA before 2013 was $51.5\% \pm 23.0\%$, and since 2013, that percentage has decreased to a median percentage of 17.6 (IQR, 8.8-36.2). This is a median of 38.3 cGy·cm²/kg (IQR, 26.4-44.3) in 2011 and 2012 and 6.7 cGy·cm²/kg (IQR, 4.7-9.2)

Table 1. Demographic data

Characteristic	N = 86
Male sex	56 (65.1%)
Primary CHD diagnosis	
Hypoplastic left heart syndrome	19 (22.1%)
PA VSD	14 (16.3%)
Hypoplastic left heart complex	9 (10.5%)
Tetralogy of Fallot	5 (5.8%)
Truncus arteriosus communis	4 (4.7%)
Hypoplastic aortic arch	4 (4.7%)
PA IVS	3 (3.5%)
Taussig-Bing	3 (3.5%)
Tricuspid atresia	3 (3.5%)
Scimitar	2 (2.3%)
Ventricular septal defect	2 (2.3%)
ccTGA	2 (2.3%)
Left pulmonary artery coarctation	2 (2.3%)
Other	14 (16.2%)
Comorbidities	
None	50 (58.1%)
Genetic syndrome	21 (24.4%)
Undefined	5 (5.8%)
Trisomy 21	2 (2.3%)
22q11	5 (5.8%)
CHARGE	2 (2.3%)
Turner	2 (2.3%)
Other	5 (5.8%)
Other	34 (39.5%)
Prematurity	9 (10.5%)
Dysmaturity	13 (15.1%)
Necrotizing enterocolitis	5 (5.8%)
Intraventricular hemorrhage	1 (1.2%)
Heart failure	1 (1.2%)
Other	5 (5.8%)

Values are n (%).

ccTGA, congenitally corrected transposition of the great arteries; CHARGE, coloboma, heart defects, atresia choanae, growth retardation, genital abnormalities, and ear abnormalities; CHD, congenital heart disease; IVS, intact ventricular septum; PA, pulmonary atresia; VSD, ventricular septal defect.

after 2012 (Figure 3). The total amount of radiation per kilogram of body weight was a median DAP of 25.8 cGy·cm² (IQR, 14.9–52.8) in diagnostic procedures and 54.3 cGy·cm² (IQR, 32.1–113.4) in interventional procedures. The proportion of radiation derived from 3DRA was a median of 8.9 cGy·cm² (IQR, 6.3–14.3) for diagnostic procedures and 6.2 cGy·cm² (IQR, 4.1–9.4) for interventional procedures.

Nine 3DRA scans were performed without use of contrast agent to visualize the stent–airway interaction postintervention. The median amount of contrast agent used in the initial 3DRA scans of the remaining procedures was 28.5 mL (IQR, 21.0–36.0). In all but 2 cases, the contrast was diluted with water to minimize contrast dye consumption. A contrast dilution ratio of 60% saline to 40% contrast agent was used in 68.8% of the performed 3DRA scans. Because of the dilution, the median amount of pure contrast was 18.0 mL (IQR, 12.7–21.6), which translates to a mean of 4.8 ± 1.6 mL/kg body weight. Contrast was

simultaneously administered at 1 to 3 locations. Most frequently, 2 contrast locations were used. The most common location for contrast administration was the RV (67 times), followed by the LV (36 times) and ascending aorta (35 times). Other possible administration locations were both atria, the venous system, or the patient's shunt.

3DRA was performed with RVP in 85 cases (78.0%). The median pace was 220/min (IQR, 210–230). The most frequently used location for RVP was the RV (65 cases, 76.5%). Other possible pacing locations were the LV, both atria, esophagus, or the patient's pacemaker.

Binary logistic regression analysis

Statistical analyses demonstrated outliers in fluoroscopy time, total radiation exposure, 3DRA-derived radiation exposure, and in the total amount of pure contrast agent used per kilogram of body weight. Multivariate binary logistic regression analysis revealed the presence of comorbidity in a patient to be significantly associated with having lower odds of receiving a 3DRA-derived radiation dose of >15 cGy·cm², with an odds ratio (OR) of 0.12 (*P* = .01). In addition, the interval between surgery and catheterization was independently associated (OR, 1.02) with a contrast dye consumption of >6 mL/kg (*P* = .046). There were no statistically significant predictors associated with a fluoroscopy time >50 minutes or high radiation exposure in the complete procedure (*P* > .05).

3DRA evaluation

In 77 (70.6%) catheterizations, 3DRA led to important additional findings. Typical new findings were unexpected vessel stenoses or identification of a native pulmonary artery system.

Discussion

Over the last decade, corrective or palliative cardiac surgery in complex CHD is applied at an early age and often in the neonatal period. Surgical outcomes in small infants have improved tremendously, for example, in palliation of HLHS¹⁰ or neonatal Ross-Konno surgery.¹¹ However, complex surgery potentially leads to complex residual lesions,¹² which can be addressed by catheter interventions. Most of the residual defects after neonatal surgery on pulmonary or systemic vessels are a result of suboptimal anastomosis, hypoplasia, or interacting structures. Some CHD lesions can be treated percutaneously at first instance (before surgery), for example, in pulmonary atresia with radiofrequency opening and stenting of the right ventricular outflow tract (RVOT).¹³

Multimodality imaging prior to catheterization and advanced imaging techniques during cardiac catheterization are crucial for procedural guidance (Central Illustration). 3DRA is an advanced technology, performing CTA during cardiac catheterization with computational conversion of rotational angiography into a volume-rendered data set.¹⁴ The volume-rendered data set offers high spatial resolution, accounting for tissue characteristics with different Hounsfield unit ranges. Topographic interactions of different types (vessel–vessel, vessel–airway, vessel–bone) are visualized identically to CTA.¹⁵ Advanced guidance of interventional procedures is facilitated by back projection of the 3D image as a 3D roadmap on the conventional angiographic system. CTA and magnetic resonance imaging data can be imported and used to guide interventions alternatively or complementary to a 3DRA.^{16,17} In clinical practice, standards in 3DRA protocols are necessary to address the location and amount of contrast injection, RVP and overall timing. However, the use of 3DRA is still underrated due to concerns of radiation exposure, complexity of the workflow, and safety in hemodynamically unstable infants.

Table 2. Patient characteristics in all procedures

Total procedures	N = 109
Interventional procedures	62 (56.9%)
Age, d	50.0 (20.0–98.5)
Weight, kg	3.8 (3.2–4.5)
Univentricular	44 (40.4%)
Diagnosis categories	
Hypoplastic left heart syndrome	31 (28.4%)
Tetralogy of Fallot	32 (29.4%)
Aortic lesions	14 (12.8%)
Diverse	32 (29.4%)

Values are n (%) or median (IQR).

Table 3. Catheterization details

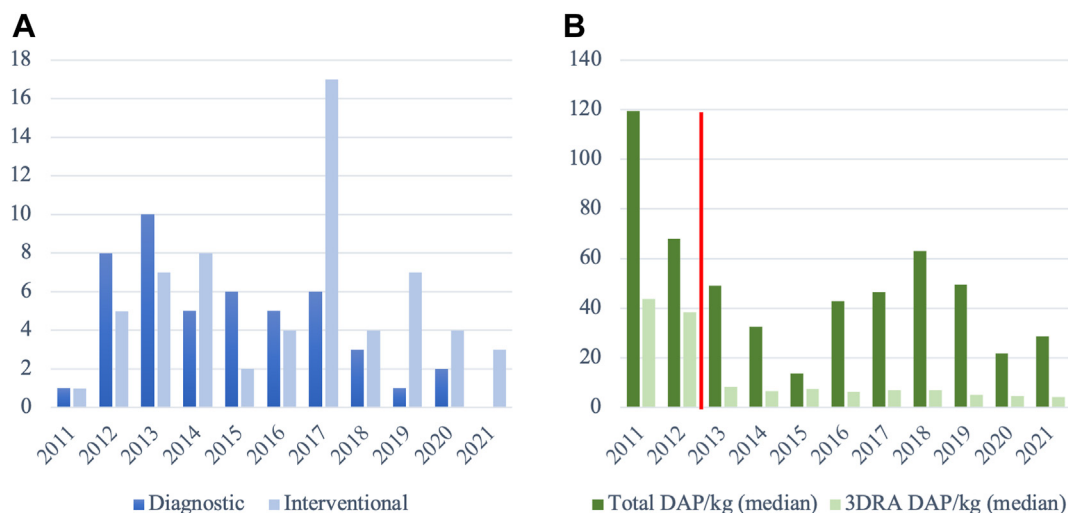
	Total (N = 109)	HLHS (n = 31)	TOF (n = 32)	AO (n = 14)	P
State of CC					0.42
Emergency	54 (49.5%)	19 (59.4%)	15 (53.1%)	7 (50%)	
Electively	55 (50.5%)	12 (40.6%)	17 (46.9%)	7 (50%)	
Reason for 3DRA					0.03
Anatomy	23 (21.1%)	3 (9.7%)	7 (21.9%)	2 (14.3%)	
Guidance	46 (42.2%)	13 (41.9%)	16 (50%)	6 (42.9%)	
Cyanosis	14 (12.8%)	9 (29.0%)	3 (42.9%)	0 (0%)	
Heart failure	7 (6.4%)	0 (0%)	1 (0%)	2 (14.3%)	
Prior to surgery	19 (17.4%)	6 (19.4%)	5 (14.3%)	4 (18.6%)	
Intervention	62 (56.9%)	20 (64.5%)	20 (62.5%)	8 (57.1%)	0.33
Type of intervention					0.00
PA stenting	14 (12.8%)	2 (6.5%)	4 (12.5%)	2 (14.3%)	
Shunt stenting	14 (12.8%)	10 (32.3%)	1 (3.1%)	0 (0%)	
Aorta dilation	8 (7.3%)	3 (9.7%)	1 (3.1%)	3 (21.4%)	
Embolization	9 (8.3%)	2 (6.5%)	2 (6.3%)	1 (7.1%)	
PA HF opening	5 (4.6%)	0 (0%)	5 (15.6%)	0 (0%)	
RVOT stenting	4 (3.7%)	0 (0%)	4 (12.5%)	0 (0%)	
Divers	8 (7.3%)	3 (9.7%)	3 (9.4%)	2 (14.3%)	
Procedure duration, min					0.94
Overall	130.0 (90.0–195.0)	120.0 (90.0–195.0)	155.0 (77.5–206.3)	120.0 (70.8–195.0)	
Interventional	175.0 (120.0–273.0)	175.0 (120.0–237.5)	163.5 (100.0–320.0)	155.0 (120.0–322.5)	
Diagnostic	90.0 (70.0–130.0)	90.0 (60.0–120.0)	97.5 (71.3–175.0)	80.5 (56.3–112.5)	
Fluoroscopy time, min					0.25
Overall	25.0 (14.4–49.9)	24.9 (16.2–45.4)	33.1 (16.5–61.5)	16.1 (13.1–43.8)	
Interventional	40.1 (25.7–65.1)	30.8 (22.8–47.9)	53.45 (20.7–93.1)	31.4 (14.8–71.5)	
Diagnostic	15.9 (7.5–20.2)	14.4 (3.7–22.6)	22.0 (11–31.8)	15.4 (9.4–16.1)	
Surgery prior to CC	59 (54.1%)	29 (93.5%)	8 (25.0%)	8 (57.1%)	0.00
Interval surgery - CC	47.6 ± 36.5	40.3 ± 31.7	57 ± 32.7	59 ± 35.5	0.47
Fluoroscopy time ≥50 min	27 (24.8%)	5 (16.1%)	3 (21.4%)	11 (34.4%)	0.40
Total DAP/kg ≥100	20 (18.3%)	7 (22.6%)	8 (25.0%)	1 (7.1%)	0.36
Total 3D DAP/kg ≥15	16 (14.7%)	2 (6.5%)	2 (14.3%)	4 (12.5%)	0.21
Contrast agent/kg ≥6	25 (25%)	6 (20.0%)	1 (8.3%)	11 (37.9%)	0.19

Normally distributed variables are expressed as mean ± SD, others as median (IQR). Categorical variables are expressed as n (%).

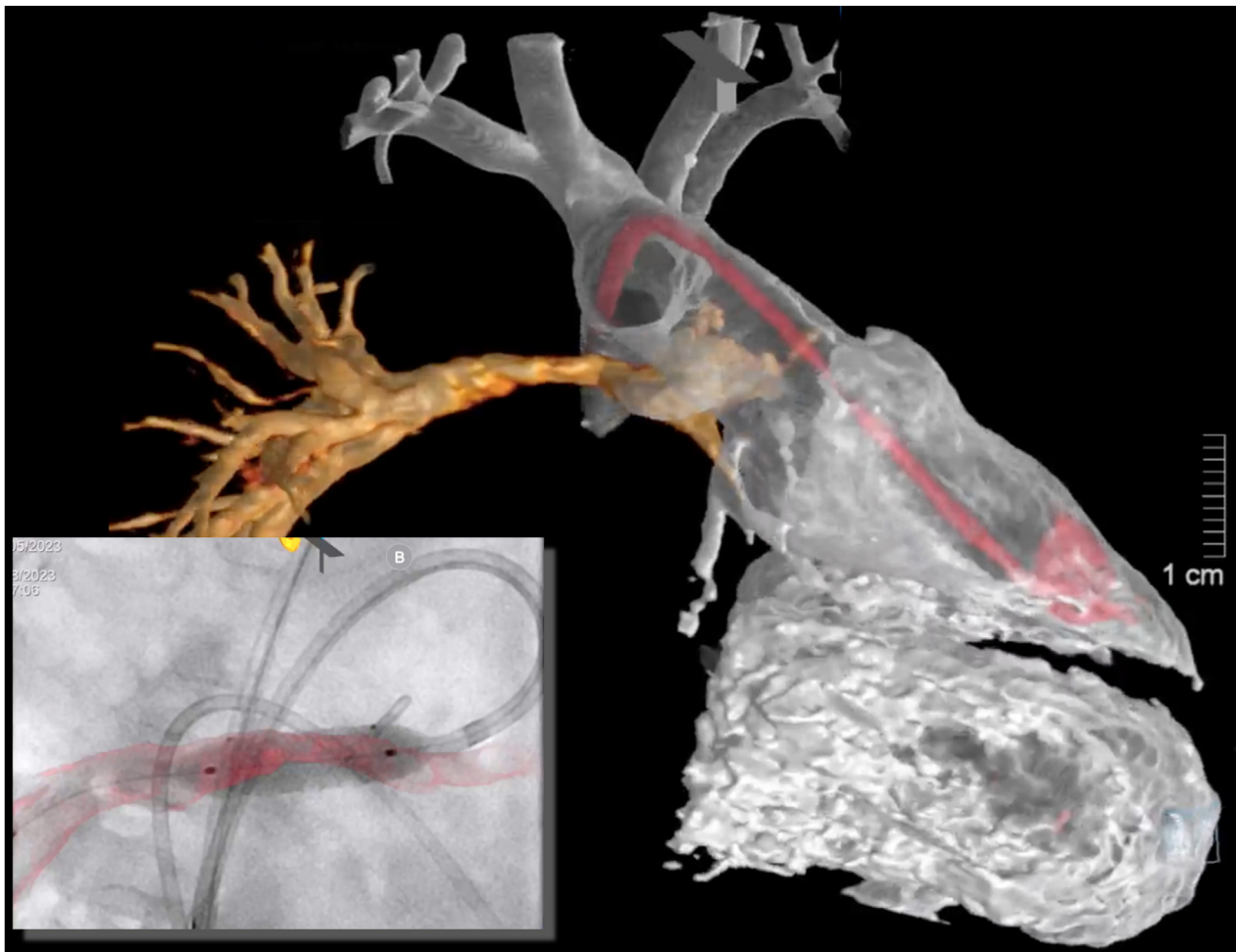
3DRA, 3-dimensional rotational angiography; AO, aortic lesions; CC, cardiac catheterization; DAP, dose area product; HF, heart failure; HLHS, hypoplastic left heart syndrome; PA, pulmonary artery; RVOT, right ventricular outflow tract; TOF, tetralogy of Fallot.

This retrospective study reports a single center experience of the use of 3DRA during cardiac catheterizations in small infants with CHD weighing <5 kg. There are few publications on cardiac catheterizations in children weighing <5 kg. In a retrospective, national, multicenter study, Giordano et al¹⁸ reported over 1600 interventional procedures performed over an 8-year period. Rashkind procedures (42.8%), arterial duct stenting (13.1%), balloon pulmonary or aortic valvuloplasty

(30.3%), and atretic pulmonary valve perforations (7.8%) made up the majority of the interventions in their study. RVOT perforation was the only intervention in the study by Giordano et al¹⁸ that would typically be considered eligible for 3DRA guidance. In our cohort, 3DRA was mostly used in pulmonary artery, aortic, or shunt stenoses requiring stent implantation or in embolization of large collateral vessels. These indications were not represented in the Italian study, which resulted in

**Figure 3.**

Procedural characteristics over the study period of 10 years: November 2011 to April 2021. (A) The amount of diagnostic procedures versus interventional procedures. Since 2018, there has been a significant reduction in procedures performed for diagnostic purposes only. (B) The median radiation dose (dose area product: cGy·cm²) per kilogram in the entire procedure versus solely derived from 3D rotational angiography. The red vertical line indicates the moment of major adaptations to limit radiation exposure.



Central Illustration.

Three-dimensional rotational angiography to visualize central shunt to right pulmonary artery stenosis and to guide stent implantation in single ventricle morphology in a 3.8 kg child.

different cohorts and results. Nicholson et al¹⁹ conducted a single-center, retrospective cohort study on cardiac catheterization performed in the early postoperative period in children with CHD. The median weight (5.2 kg) of their participants was above our maximum inclusion weight, which makes it inappropriate to compare results. The largest cohort study on the use of 3DRA in pediatric patients with CHD was conducted by Söder et al.⁵ Their patients in their study had a median weight of 14.2 kg (IQR, 7.4-42.5), which was also substantially higher than that of our cohort. However, there are no publications on 3DRA usage during cardiac catheterizations in children with <5 kg body weight. Additionally, nearly half (49.5%) of the cardiac catheterization procedures in our cohort were performed in a state of emergency, which makes finding comparable cohort studies even more challenging.

In our study, 86 patients underwent 109 cardiac catheterizations with the use of 3DRA. The population included in this study is characterized by a high percentage of emergency indications (49.5%) in a complex group of children with a body weight <5 kg. Most of them underwent cardiac catheterization after previous cardiac surgery. The median weight of our study population was 3.8 kg. Predominant diagnoses were HLHS, aortic lesions, and Fallot-like abnormalities. These predominant diagnoses alone already account for >70% of the patients, which demonstrates the complexity in our cohort. The anatomical variances and difficulties were significant, which makes delineation of the vessel geometry crucial to understand the target lesion. 3DRA allows for unrestricted virtual angulation of the target lesion, which is not

achievable when using regular biplane angiography. Additionally, 3D guidance during interventional procedures is particularly beneficial. Figure 2 illustrates examples of 3 patients in which 3DRA made a substantial difference. The first case concerns an infant with HLHS weighing 3.8 kg who developed severe cyanosis and cardiac failure 10 days after a Norwood procedure. Despite maximum therapeutic efforts, his oxygen saturation levels persisted below 50%. Biplane angiography in extreme angulations could not visualize the problem. Additionally, ultrasonography in these small and critically ill children can only demonstrate turbulence of blood flow but is not accurate enough to depict the details and specific location of stenoses. Despite the hemodynamically unstable conditions, 3DRA was performed safely. Only virtual angulation from a caudal view could generate the unrestricted view of the severe Sano shunt to right pulmonary artery (RPA) stenosis. Implantation of a coronary stent was performed with the use of 3DRA guidance, after which the infant stabilized rapidly. In the second case, 3DRA was essential to guide recanalization of the occluded RPA 6 weeks after correction of a transverse aortic constriction. A telescopic system within a 7F steerable Ocosor sheath was precisely guided with the use of 3DRA, allowing penetration of the occluded ostium and stent implantation, which resulted in re-established RPA perfusion. The third case demonstrates stenting of a patent ductus arteriosus under 3DRA guidance in a newborn weighing 3.6 kg with PA VSD and absence of a native pulmonary artery system.

The use of 3DRA in children with CHD and a body weight <5 kg proved to be safe. VF was induced by RVP in 2 patients with high RV

pressure load as a result of severe pulmonary artery branch stenoses. This corresponds to our experience with 3DRA in older children and adults. Therefore, in patients with impaired ventricular function and low cardiac output, RVP is not indicated. However, creating awareness of the potential development of VF in these patients, ensuring preparations have been made and essential equipment is within reach, can guarantee safe practice of 3DRA with RVP in these patients. Despite the high complexity and morbidity of these children, no deaths occurred during cardiac catheterizations with the use of 3DRA.

The median total DAP per kilogram in our study was 42.1 cGy·cm², of which 7.1 cGy·cm² was derived from 3DRA. Söder et al.⁵ reported a median DAP per kilogram of 16.9 cGy·cm² with 3.8 cGy·cm²/kg derived solely from 3DRA. Our workflow was based on multilocation contrast injection, in contrast to the single location contrast injection used by Söder et al.⁵ This results in more absorption of radiation due to a higher iodine concentration in the chest. Moreover, the amount of contrast applied in small infants is relatively higher than that applied in older children. This in turn causes more radiation absorption in our population compared to the one of Söder et al.⁵ (median weight 3.8 kg vs 14.2 kg). In our 3DRA learning process, major radiation adaptations were introduced in December 2012, leading to a remarkable dose reduction in 3DRA.²⁰ These adaptations included higher dilution of contrast and 50% reduction of the amount of frames per second during the rotational angiography. The 3DRA system from Siemens Healthineers⁹ comes with 2 different possible frame rates per second. The frame rates are a result of the degree of rotation per frame. This means that 60 frames per second correspond to 0.8° of rotation per frame, whereas 30 frames per second correspond to 1.5° of rotation. At our institution, a series of phantom 3DRA scans were performed using an electronic microcrocodile clamp and demonstrated the 30-frames-per-second setup to be sufficient in depicting cardiac anatomy, whereas the 60 frames-per-second setup displayed a redundant amount of detail.²⁰ As a result, a 50% reduction in the amount of radiation used in 3DRA was achieved. Additionally, we optimized the radiation presets for each weight-dependent preset. Hence, after 2012, radiation exposure during 3DRA was diminished significantly in our institution (Figure 3).

The median contrast agent used per kilogram of body weight was 4.7 mL in our study. Söder et al.⁵ described a much lower median contrast dye consumption of 1.6 mL/kg. The main reason for this difference is the predominant use of multilocation contrast administration in the Utrecht protocol. Multilocation contrast administration is used to visualize potential interactions of anatomic structures. Examples of critical interactions are the potential compression of the left bronchus in stenting of the left pulmonary artery after a Norwood procedure or left coronary artery compression due to RPA stenting after a Ross procedure. In cases of critical interactions, balloon interrogation before stenting can be applied to avoid these rare but life-threatening complications.

Multivariate binary logistic regression analysis was applied to test for predisposing factors with regard to outliers in procedural data, such as radiation dose and amount of contrast agent administered. The presence of comorbidity emerged as protective factor for receiving a high 3DRA-derived radiation dose (OR, 0.12). A possible explanation could be that genetic syndromes (included as comorbidities in this study) are less frequent in HLHS than in PA VSD, TOF, and double outlet RV. In these RVOT lesions, the amount of contrast dye used during 3DRA is focused on the pulmonary arteries. This results in less overall contrast dye administration, potentially leading to less radiation exposure. However, conclusive interpretation of this relation remains cumbersome. Furthermore, the interval between surgery and cardiac catheterization was independently associated with receiving a larger amount of contrast agent (≥ 6 mL/kg). The mechanism behind this association remains speculative, as it has not been mentioned in literature previously, and intensive clinical reasoning did not yield any possible

hypotheses. Additionally, considering its marginal OR of 1.02, no clinical significance was expected of this association. Sex, age, weight, cardiac diagnosis, state of emergency, and previous cardiac surgery were also included in the binary logistic regression analysis but were not statistically significant. This may be explained by the homogeneity of the patient population with an overall high complexity and small range of age and weight.

In our study, 3DRA was initially used more frequently for diagnostic purposes, due to a lack of a high-quality imaging CT scanner until 2017. With installation of a state-of-the-art CT scanner, the need for diagnostic 3DRA decreased and thereafter, 3DRA was predominantly used for interventional purposes (Figure 3). This workflow offers preprocedural planning and periprocedural guidance by importation of the CTA images onto the 3DRA workstation.

Despite the described advantages, there are considerable limitations to the usage of 3DRA. First, the workflow of performing and postprocessing high-quality 3DRA scans is complex and involves the entire team. Adaptation to the technique of rotational angiography is necessary, considering the extended ventilation tubes, RVP, and 180° rotation of the frontal plane around a small patient with a huge variety of monitoring elements and cables. Second, contrast administration differs substantially from conventional biplane angiography concerning contrast dilution, amount, timing, and location. Radiation dose and contrast amount of a single 3DRA scan have to be set into proportion with the equivalent of multiple conventional biplane angiographies to overcome the concerns of the team. Careful adaptations during the learning process should address radiation settings and workflow aspects to avoid unnecessary harm or insufficient imaging results. Third, volume data sets derived from 3DRA only contain static image information, whereas biplane conventional angiography is dynamic. Hence, both techniques address different and complementary types of image information. The anatomical information of the rotational angiography should be studied carefully before postprocessing the 3D volume data. Furthermore, until now, there has been no technique available to automatically correct for anatomical shifts when using 3D roadmapping. Vendors should focus on this shortcoming to initiate technical advancement in 3D roadmapping. Studies on the feasibility of 4D rotational angiography are ongoing and demonstrate promising results for dynamic 3D imaging with high spatial resolution during cardiac catheterization.²¹

The findings of this study should be interpreted in light of some limitations. This was a single center, retrospective cohort study with the usual associated disadvantages. Moreover, during the 10-year study period, there was a learning process. As a result, contrast administration, radiation exposure, and other procedural settings changed over the years, which affected the results. Additional limitations of 3DRA include loss of dynamic information and the complex workflow that comes with the technique.

Conclusion

3DRA is an advantageous periprocedural imaging technique within the field of cardiac catheterization, enabling visualization of anatomic structures, lesions, and their interactions not visible in conventional angiography. Its application in infants with <5 kg body weight, who are often hemodynamically unstable, has proven to be safe. In the time period of this study, only a few complications related to the use of 3DRA occurred, and the amount of radiation exposure and contrast dye consumption was found to be very acceptable. High-quality CTA can be used with a 3D-capable system to substitute for 3DRA. However, diagnostic 3DRA can be useful when a CT scan is inconclusive or when the patient clinically deteriorates and cardiac catheterization becomes necessary anyway. 3DRA is highly valuable in CHD to understand complex vessel lesions and to guide the interventional procedures.

Despite the limitations, usage of the technique in vulnerable, ill children with complex lesions can be exceedingly beneficial. Developing a global consensus on the use of 3DRA in small infants and creating standardized procedure protocols is desirable and necessary.

Declaration of competing interest

Gregor J. Krings is a member of the advisory board of Siemens Healthineers. The remaining authors declared no potential conflicts of interest with respect to the research, authorship, and/or publication of this article.

Funding sources

This work was not supported by funding agencies in the public, commercial, or not-for-profit sectors.

Ethics statement and patient consent

The research reported adhered to the relevant ethical guidelines, and patient consent was obtained.

References

1. Liu Y, Chen S, Zühlke L, et al. Global birth prevalence of congenital heart defects 1970-2017: updated systematic review and meta-analysis of 260 studies. *Int J Epidemiol*. 2019;48(2):455–463.
2. van der Linde D, Konings EE, Slager MA, et al. Birth prevalence of congenital heart disease worldwide: a systematic review and meta-analysis. *J Am Coll Cardiol*. 2011; 58(21):2241–2247.
3. Blue GM, Kirk EP, Sholler GF, Harvey RP, Winlaw DS. Congenital heart disease: current knowledge about causes and inheritance. *Med J Aust*. 2012;197(3):155–159.
4. Glatz AC, Zhu X, Gillespie MJ, Hanna BD, Rome JJ. Use of angiographic CT imaging in the cardiac catheterization laboratory for congenital heart disease. *J Am Coll Cardiol Img*. 2010;3(11):1149–1157.
5. Söder S, Wälisch W, Dittrich S, Cesnjevar R, Pfammatter JP, Glöckler M. Three-dimensional rotational angiography during catheterization of congenital heart disease - a ten years' experience at a single center. *Sci Rep*. 2020;10(1):6973.
6. Haddad L, Waller BR, Johnson J, et al. Radiation protocol for three-dimensional rotational angiography to limit procedural radiation exposure in the pediatric cardiac catheterization lab. *Congenit Heart Dis*. 2016;11(6):637–646.
7. Kehl HG, Jäger J, Kececioglu D, et al. Three dimensional X-ray angiography. Pediatric angiocardiology in three and four dimensions: evolution of methods, validation, and first clinical results. In: Imai Y, Momma K, eds. *Proceedings of the Second World Congress of Pediatric Cardiology and Cardiac Surgery*. Futura Pub Co; 1998:465–468.
8. Dose Area Product. Science Direct. Accessed May 1, 2021. <https://www.science-direct.com/topics/medicine-and-dentistry/dose-area-product>
9. Syngo DynaCT Cardiac. Siemens Healthineers. Accessed May 1, 2021. <https://www.siemens-healthineers.com/nl/angio/options-and-upgrades/clinical-software-applications/syngo-dynact-cardiac>
10. Metcalf MK, Rychik J. Outcomes in hypoplastic left heart syndrome. *Pediatr Clin North Am*. 2020;67(5):945–962.
11. Accord RE, Schoof P, Krings G, Haas F, Ross-Konno for interrupted aortic arch: simplified arch reconstruction using swing-back technique. *Ann Thorac Surg*. 2018;105(2):e91–e93.
12. Wong D, Benson LN, Van Arsdell GS, Karamlou T, McCrindle BW. Balloon angioplasty is preferred to surgery for aortic coarctation. *Cardiol Young*. 2008; 18(1):79–88.
13. Morgan GJ, Narayan SA, Goreczny S, et al. A low threshold for neonatal intervention yields a high rate of biventricular outcomes in pulmonary atresia with intact ventricular septum. *Cardiol Young*. 2020;30(5):649–655.
14. Kang SL, Armstrong A, Krings G, Benson L. Three-dimensional rotational angiography in congenital heart disease: present status and evolving future. *Congenit Heart Dis*. 2019;14(6):1046–1057.
15. Ferandos C, El-Said H, Hamzeh R, Moore JW. Adverse impact of vascular stent “mass effect” on airways. *Catheter Cardiovasc Interv*. 2009;74(1): 132–136.
16. Goreczny S, Dryzek P, Morgan GJ, Lukaszewski M, Moll JA, Moszura T. Novel three-dimensional image fusion software to facilitate guidance of complex cardiac catheterization: 3D image fusion for interventions in CHD. *Pediatr Cardiol*. 2017; 38(6):1133–1142.
17. Goreczny S, Dryzek P, Moszura T, Kühne T, Berger F, Schubert S. 3D image fusion for live guidance of stent implantation in aortic coarctation - magnetic resonance imaging and computed tomography image overlay enhances interventional technique. *Postępy Kardiologii Interwencyjnej*. 2017;13(3):269–272.
18. Giordano M, Santoro G, Agnoletti G, et al. Interventional cardiac catheterization in neonatal age: results in a multicentre Italian experience. *Int J Cardiol*. 2020;314: 36–42.
19. Nicholson GT, Kim DW, Vincent RN, Kogon BE, Miller BE, Petit CJ. Cardiac catheterization in the early post-operative period after congenital cardiac surgery. *J Am Coll Cardiol Interv*. 2014;7(12):1437–1443.
20. Minderhoud SCS, van der Stelt F, Molenschot MMC, Koster MS, Krings GJ, Breur JMPJ. Dramatic dose reduction in three-dimensional rotational angiography after implementation of a simple dose reduction protocol. *Pediatr Cardiol*. 2018; 39(8):1635–1641.
21. Taubmann O, Haase V, Lauritsch G, et al. Assessing cardiac function from total-variation-regularized 4D C-arm CT in the presence of angular undersampling. *Phys Med Biol*. 2017;62(7):2762–2777.